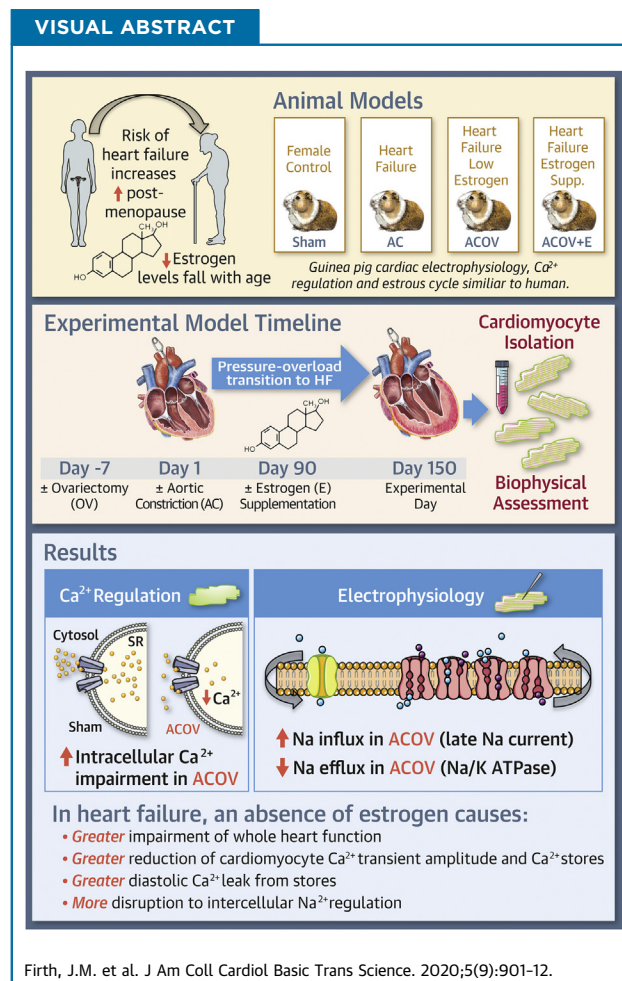


PRECLINICAL RESEARCH

The Effect of Estrogen on Intracellular Ca^{2+} and Na^{+} Regulation in Heart Failure



Jahn M. Firth, PhD,^a Hsiang-Yu Yang, MD, PhD,^b Alice J. Francis, BSc,^a Najah Islam, BSc,^a Kenneth T. MacLeod, PhD^a



HIGHLIGHTS

- During the progression toward heart failure, indicators of in vivo whole-heart function suggest greater impairment in the absence of estrogen.
- At the single cardiac myocyte level, the absence of estrogen results in further reduction of Ca^{2+} transient amplitudes, further slowing of transient decay kinetics, less SR Ca^{2+} content, and a further increase in Ca^{2+} spark frequencies and spark-mediated SR leak compared with animals with normal estrus cycles.
- Cardiac myocyte Na^{+} regulation is also more disrupted in the absence of estrogen.

ABBREVIATIONS AND ACRONYMS

AC = aortic constriction

ACOV = aortic constriction
with ovariectomy

ACOV+E = aortic constriction
with ovariectomy,
supplemented with 17 β -
estradiol

FS = fractional shortening

I_{Ca} = L-type Ca^{2+} channel
current (cadmium-sensitive)

$I_{Na,L}$ = late Na^{+} current
(ranolazine-sensitive)

NCX = Na^{+}/Ca^{2+} exchange

OV = ovariectomy

SERCA = Sarco/endoplasmic
reticulum Ca^{2+} -ATPase

SR = sarcoplasmic reticulum

SUMMARY

Contradictory findings of estrogen supplementation in cardiac disease highlight the need to investigate the involvement of estrogen in the progression of heart failure in an animal model that lacks traditional comorbidities. Heart failure was induced by aortic constriction (AC) in female guinea pigs. Selected AC animals were ovariectomized (ACOV), and a group of these received 17 β -estradiol supplementation (ACOV+E). One hundred-fifty days post-AC surgery, left-ventricular myocytes were isolated, and their electrophysiology and Ca^{2+} and Na^{+} regulation were examined. Long-term absence of ovarian hormones exacerbates the decline in cardiac function during the progression to heart failure. Estrogen supplementation reverses these aggravating effects. (J Am Coll Cardiol Basic Trans Science 2020;5:901-12) © 2020 The Authors. Published by Elsevier on behalf of the American College of Cardiology Foundation. This is an open access article under the CC BY-NC-ND license (<http://creativecommons.org/licenses/by-nc-nd/4.0/>).

Sex differences in the incidence and progression of cardiovascular diseases are widely documented (1), and although some of the underlying mechanisms are beginning to be established (2), there remain large knowledge gaps, probably as a result of the complexity of comorbidities such as diabetes, hypertension, chronic obstructive pulmonary disease (COPD), coronary artery disease, and peripheral vascular disease.

The prevalence of cardiovascular diseases, particularly heart failure, increases with age in both men and women but shows a more prominent increase in women older than 50 years of age. Part of the underlying reason has been thought to be caused by a decline in estrogens around menopause (3), but distinguishing between the effects of the menopause per se, biological aging processes and comorbidities is challenging, and therefore estrogen involvement in the mechanisms associated with the progression of heart failure remains controversial. Further, the failure of large clinical trials examining the effects of hormone replacement therapy on the cardiovascular health of post-menopausal women (4,5) to show consistent benefit halted the drive for progress in the area, but, since then, it has emerged that the medication used and the targeted age for therapy were not

optimal (6), and it has become clearer that women who experience premature or early-onset menopause have a greater risk of cardiovascular mortality (7).

We have previously shown that the long-term absence of ovarian hormones in the guinea pig leads to detrimental changes to intracellular Ca^{2+} regulation in the heart, resulting in the formation of a proarrhythmic substrate (8). Studies on mice support the idea of Ca^{2+} dysregulation following ovariectomy (9,10), and, in rats, it has been shown that estrogen can reduce incidence of arrhythmia following episodes of ischemia reperfusion (11). Postmenopausal women are more vulnerable to arrhythmia-related sudden cardiac death compared with pre-menopausal women (12).

It is important to understand why these sex differences arise because prevention and management of cardiovascular disease may benefit from sex-specific approaches.

The aim of this study was to characterize the influence of estrogen on cardiac function during the onset of heart failure in a controlled animal model that lacks traditional comorbidities. The guinea pig offers an appropriate model because it shares similar electrophysiological, Ca^{2+} regulatory, and steroidogenesis features with humans (13), and a well-characterized model of heart failure in this species exists (14).

From the ^aNational Heart and Lung Institute, Imperial College, Hammersmith Hospital, London, United Kingdom; and ^bCardiovascular Surgery, Tri-Service General Hospital, National Defense Medical Center, Taipei, Taiwan (R.O.C.). This work was supported by the British Heart Foundation [Project Grant Number: PG/032/27241], London, United Kingdom, to Dr. MacLeod. Dr. Yang has received funding from Tri-Service General Hospital, National Defense Medical Center, Taipei, Taiwan (R.O.C.). All other authors have reported that they have no relationships relevant to the contents of this paper to disclose.

The authors attest they are in compliance with human studies committees and animal welfare regulations of the authors' institutions and Food and Drug Administration guidelines, including patient consent where appropriate. For more information, visit the JACC: Basic to Translational Science [author instructions page](#).

Manuscript received March 26, 2020; revised manuscript received June 22, 2020, accepted June 23, 2020.

METHODS

ETHICAL APPROVAL. All studies were carried out with the approval of the Animal Welfare and Ethical Committee of Imperial College London and the Home Office, United Kingdom, and are in accordance with the United Kingdom Home Office Guide on the Operation of the Animals (Scientific Procedures) Act 1986, which conforms to the Guide for the Care and Use of Laboratory Animals published by the US National Institutes of Health under assurance number A5634-01.

ANIMAL MODEL. In an animal whose cardiac cell physiology closely resembles that of the human, we have established pressure-overload heart failure that replicates many of the in vivo and cellular features observed in the human condition (14). Here, we extended the model by using female Dunkin-Hartley guinea pigs (350 g to 450 g, Marshall BioResources, Hull, United Kingdom) to examine the effects of long-term absence of ovarian hormones on heart failure. Four experimental groups were generated: sham-operated control, transaortic constriction (AC), transaortic constriction with ovariectomy (ACOV), and transaortic constriction with ovariectomy supplemented with 17 β -estradiol (ACOV+E). Animals initially underwent ovariectomy (OV) through a bilateral flank approach, in which both ovaries were surgically removed (8). A minimum of 7 days between the OV and AC procedures allowed appropriate recovery. In the ACOV group, selected animals received 60-day release pellets, containing 1 mg 17 β -estradiol (Innovative Research of America, Sarasota, Florida) that was implanted subcutaneously in the back region 90 days following ovariectomy surgery. Animals received the same pre-medication and post-recovery treatment for the AC, OV, and 17 β -estradiol- supplementation procedures. The pre-medication comprised the anticholinergic agent atropine (0.05 mg/kg subcutaneously), prophylactic antibiotic enrofloxacin (5 mg/kg subcutaneously), a nonsteroidal anti-inflammatory carprofen (5 mg/kg subcutaneously), partial agonist opioid buprenorphine (0.05 mg/kg subcutaneously) and metoclopramide (0.5 mg/kg subcutaneously) to aid gut motility following surgery. A local anesthetic bupivacaine (2 mg/kg subcutaneously) was injected around the incision site. Intraoperative hydration was provided with 4 ml/kg/h saline 0.9% subcutaneously, and general anesthesia was maintained with 2% to 3% isoflurane. Immediately after surgery, animals were placed in a recovery chamber maintained at 30°C (86°F) and with an environment of 100% oxygen.

Animals were housed in separate cages following surgery, receiving 0.05 mg/ml carprofen in their drinking water for 72 h to maintain post-surgery analgesia, and then returned to their cages of origin with environment enrichment. Animals were housed for 150 days post AC or OV procedures at 69.8 \pm 1.8°F (33.8°F) in a controlled lighting environment (12-h light-dark cycles) and were provided with standard guinea pig feed and water ad libitum. Ovariectomized animals were provided with a casein-based, soy-free diet to minimize the uptake of phytoestrogens.

M-MODE ECHOCARDIOGRAPHY. In vivo cardiac function was measured by echocardiography performed on unanesthetized animals to overcome anesthetic drug influences on heart function as described in Ke et al. (14).

MYOCYTE ISOLATION. Heart and lungs were rapidly explanted from the thorax of anesthetized animals and placed in ice-cold Krebs-Henseleit solution (for composition, see [Supplemental Material](#)) containing 500 IU heparin sodium and weighed separately. Single left-ventricular myocytes were enzymatically isolated from Sham, AC, ACOV, and ACOV+E hearts, as previously described (8,14,15), then resuspended in Dulbecco's modified Eagle's medium solution (Gibco BRL, ThermoFisher Scientific, Waltham, Massachusetts) at room temperature and used within 6 to 8 h. Cells with rounded edges, obvious cytoplasmic vesicles, automatic activity before stimulation, major ultrastructural defects, absence of clear striations or cells that were not incompletely isolated (e.g., cell pairs) were not used.

INTRACELLULAR CA²⁺ MEASUREMENTS. Cells were superfused with normal Tyrode's solution (for composition, see [Supplemental Material](#)) at 37°C (98.6°F). Caffeine and Na⁺-free, Ca²⁺-free solution were superfused when required in protocols as described in Ke et al. (14) and Yang et al. (8). A line-scanning confocal microscope with a BioRad Radiance 2000 (Central Microscopy Research Facility, University of Iowa, Iowa City, Iowa) attachment with our published recording parameters (8,14,16) was used to record Ca²⁺ sparks. Raw images were analyzed using the ImageJ SparkMaster (National Institutes of Health, Bethesda, Maryland) plugin (17) and custom macros (16), with the detection criteria set to 4.2 standard deviations (SDs) above the mean background value. Spark frequency, amplitude, full-width at half maximum (FWHM), and full-duration at half maximum (FDHM) were measured. Spark mass was calculated as previously described (18).

TABLE 1 Physical Characteristics of the Experimental Animal Groups

Model	Sham (n = 9)	AC (n = 9)	ACOV (n = 6)	ACOV+E (n = 6)
Body weight (g)	783.6 ± 21.36	774.2 ± 18.91	778.9 ± 24.00	751.4 ± 12.87
HW:BW (g/kg)	3.10 ± 0.08‡	4.83 ± 0.14†‡	5.35 ± 0.11†	4.71 ± 0.26†‡
LW:BW (g/kg)	4.31 ± 0.09‡	5.30 ± 0.24†‡	6.40 ± 0.37†	5.71 ± 0.18†‡
UW:BW (g/kg)	1.99 ± 0.57‡	2.06 ± 0.49‡	0.53 ± 0.19†	5.69 ± 0.94†‡
Serum E2 (pg/ml)	7.80 ± 4.36‡	8.20 ± 3.60‡	4.0 ± 1.90*	30.1 ± 10.0†‡
LVIDd (cm)	0.67 ± 0.07‡	0.77 ± 0.08†	0.78 ± 0.05†	0.73 ± 0.04*
LVIDs (cm)	0.26 ± 0.03‡	0.41 ± 0.03†‡	0.47 ± 0.04†	0.40 ± 0.06†‡
FS (%)	60.8 ± 2.88‡	46.3 ± 4.54†‡	39.7 ± 3.31†	45.5 ± 5.25†‡

Values are mean ± SD. Heart weight (HW), lung weight (LW), uterine weight (UW), body weight (BW), and serum (E2) 17β-estradiol. In vivo M-mode echocardiography measurements of the left-ventricle internal diameter end diastole (LVIDd) and end systole (LVIDs). Fractional shortening (FS) was significantly reduced in all 3 failing groups compared with Sham and was further reduced in ACOV compared with the AC (±E) groups. The notation describing p values is as follows: *p < 0.05 and †p < 0.001 when comparisons were made with the Sham group. When comparisons were made with the ACOV group the notation describing p values is ‡p < 0.05.

AC = aortic constriction; ACOV = aortic constriction with ovariectomy; ACOV+E = aortic constriction with ovariectomy supplemented with 17β-estradiol.

SINGLE-CELL ELECTROPHYSIOLOGICAL MEASUREMENTS.

Sharp microelectrodes (20–40 MΩ) were used to record action potentials, Na⁺/Ca²⁺ exchange (*I*_{NCX}) and L-type Ca²⁺ channel (*I*_{Ca,L}) currents, using a switch-clamping system (Axoclamp 2B Amplifier, Molecular Devices, LLC, San Jose, California). Late Na⁺ (*I*_{Na,Late}) and Na⁺/K⁺ ATPase currents were measured in the whole-cell configuration using patch pipettes (with resistances 4–7 MΩ when filled with their pipette solutions). The protocols for these electrophysiological measurements are detailed in Ke et al. (14). During the electrophysiological experiments, myocytes were superfused with normal Tyrode's solution at 37°C, except during the recordings of *I*_{Na,Late}, which were at room temperature. *I*_{Na,Late} was evaluated as ranolazine-sensitive current.

SERUM 17β-ESTRADIOL. Blood samples (2 to 3 ml) from the inferior vena cava were collected and stored in serum separator tubes (BD, Vacutainer, SST, II tubes, Franklin Lakes, New Jersey) at room temperature for a minimum of 2 h to coagulate before centrifugation at 1,300 g for 15 min at 4°C (39.2°F). The serum supernatant was collected and immediately stored at -80°C (-112°F) until assayed. A quantitative sandwich ELISA (MyBioSource Inc., San Diego, California) was performed to measure the levels of serum 17β-estradiol.

WESTERN BLOT. Protein expression for Na⁺/K⁺ ATPase and phospholemman were determined by Western blot, using protocols described in Ke et al. (14).

DATA STORAGE AND STATISTICAL ANALYSES. Fluorescence and electrophysiological data were acquired using AxoScope and ClampEx, respectively, and analyzed using Clampfit (pClamp suite v10.6,

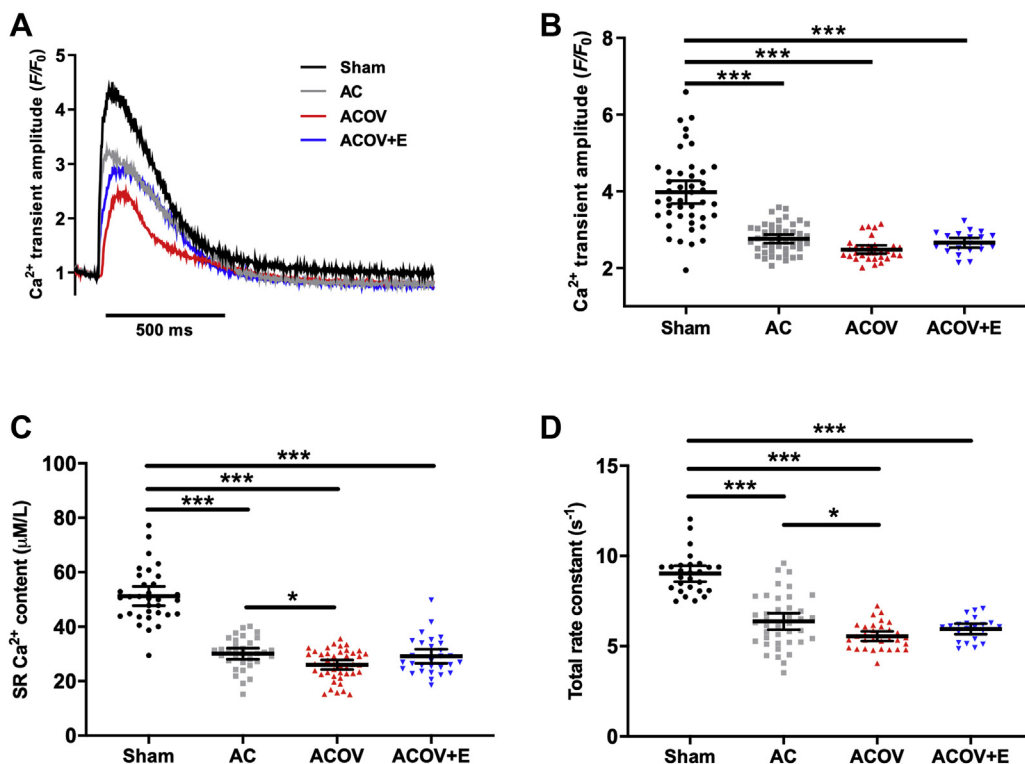
Molecular Devices, LLC, San Jose, California). Raw data were stored in Excel and transferred to GraphPad Prism 7 (GraphPad Software, San Diego, California) for statistical analyses and generation of figures. Statistical differences among means were calculated using either a 2-tailed unpaired Student's *t*-test or a 1-way analysis of variance (ANOVA) with Fisher post hoc test when we made planned comparisons and a 1-way ANOVA with a post hoc Tukey test to control for multiple comparisons when these were not planned. The test used is stated in the Figure legends. Ca²⁺ spark data, amplitude, mass, and spark-mediated sarcoplasmic reticulum (SR) leak, which were not normally distributed, were log transformed. All data are presented as mean ± SD or mean (95% confidence interval [CI] with "n" being the total number of cells from "N" the total number of hearts (n/N = cells/hearts). The p value determined to be statistically significant is p < 0.05. The notation describing p values is as follows: *p < 0.05, **p < 0.01, and ***p < 0.001, and when comparisons were made with the ACOV group, the notation describing p values is ‡p < 0.05, †‡p < 0.01, and †††p < 0.001. The number of animals in each group were Sham = 9, AC = 9, ACOV = 6, and ACOV+E = 6.

RESULTS

PHYSICAL CHARACTERISTICS OF EXPERIMENTAL ANIMALS.

In total, 30 animals were used to investigate the effect of ovarian hormones on in vivo cardiac function and intracellular Ca²⁺ and Na⁺ regulation during heart failure. At the end of the 150-day period, key physical characteristics of the experimental animals were measured and are listed in Table 1. Validation of a low estrogen environment was assessed by uterine weight and serum 17β-estradiol levels. The ACOV group had a significant 3.8-fold reduction in uterine weight relative to body weight (UW:BW ratio) and a 2.0-fold decrease in 17β-estradiol levels compared with the Sham-operated group (p < 0.001 and p < 0.05, respectively). The UW:BW and 17β-estradiol levels were unaltered in the AC group compared with Sham but significantly increased in the 17β-estradiol-supplemented group (ACOV+E). HW:BW ratio significantly increased in all 3 heart failure groups (AC, ACOV, and ACOV+E) by 56%, 73%, and 52% (p < 0.001), respectively, compared with the age-matched Sham. Pulmonary edema, typically associated with heart failure, was inferred by the increase in lung weights in the AC, ACOV, and ACOV+E groups by 23%, 49%, and 33% (p < 0.001), respectively, compared with the Sham group. In the absence of ovarian hormones (ACOV), HW:BW and LW:BW ratios were further increased compared with the AC

FIGURE 1 The Effect of Heart Failure and Long-Term Absence of Estrogen on Ca^{2+} Transient Amplitude



(A) Representative Ca^{2+} transient traces from Fluo-4-loaded myocytes. (B) All AC groups had significantly lower transient amplitudes compared with the Sham group. The Ca^{2+} transient amplitude was further reduced by 10% in ACOV compared with the AC group (Sham, $n = 44/3$ cells; AC, $n = 47/3$; ACOV, $n = 31/3$; ACOV+E, $n = 21/3$; 1-way analysis of variance (ANOVA) with a Tukey's multiple comparisons test, $***p < 0.001$). (C) Measurement of total SR Ca^{2+} content through integration of the caffeine-induced inward NCX current. Myocytes from failing hearts were characterized by a significant decrease in SR Ca^{2+} content compared with Sham ($p < 0.001$). The long-term absence of ovarian hormones further reduced SR Ca^{2+} (ACOV). (Sham, $n = 33/3$; AC, $n = 34/4$; ACOV, $n = 42/3$; ACOV+E, $n = 29/3$; 1-way ANOVA with a Fisher post hoc test: $*p < 0.05$, $**p < 0.01$, $***p < 0.001$). Bars show mean (95% confidence interval). AC = aortic constriction; ACOV = aortic constriction with ovariectomy; ACOV+E = aortic constriction with ovariectomy supplemented with 17 β -estradiol.

and ACOV+E groups by 11% and 14% (HW:BW), respectively, and 21% and 12% (LW:BW), respectively. When estrogen was supplemented (ACOV+E), these ratios returned to values comparable with that of the AC gonad-intact group.

IN VIVO M-MODE ECHOCARDIOGRAPHY. No differences were observed in the end-diastolic internal diameter of the left ventricle (LVIDd) among the heart failure groups; however, the LVIDd were all enlarged by approximately 15% compared with Sham ($p < 0.001$). The deficiency of ovarian hormones significantly increased the end-systolic internal diameter (LVIDs) in failing hearts and resulted in a 20% reduction in fractional shortening (FS) compared with the Sham group ($p < 0.001$). Together with the increased HW:BW and LW:BW ratios, the reduction in

FS illustrates the worsening of in vivo indices of pathophysiological changes occurring in pressure overload-induced heart failure, when circulating ovarian hormones are in much lower concentration. Estrogen supplementation (ACOV+E) restored the in vivo cardiac function and HW:BW and LW:BW ratios to values comparable with the AC gonad-intact group.

INTRACELLULAR Ca^{2+} CHANGES IN RESPONSE TO ELECTRICAL STIMULATION AND CAFFEINE. An important indicator of changes in intracellular Ca^{2+} regulation is the morphology of the Ca^{2+} transient during beat-to-beat stimulation (Figure 1). Fluo-4-loaded myocytes from failing hearts (AC) were characterized by a 31% reduction in Ca^{2+} transient amplitude compared with the Sham-operated group ($p < 0.001$). A further 10% reduction in transient

TABLE 2 Deciphering the Rate of Ca^{2+} Removal Mechanisms Among Experimental Groups

Rate constants (s^{-1})	Sham (n = 3/27)	AC (n = 3/41)	ACOV (n = 3/31)	ACOV+E (n = 2/21)
Total decay	9.02 ± 1.10	6.37 ± 1.40*†	5.56 ± 0.70*	5.96 ± 0.70*
SERCA	6.21 ± 1.20	3.24 ± 1.10*†	2.59 ± 0.70*	2.90 ± 0.70*
NCX	2.70 ± 0.40	2.98 ± 0.70	2.86 ± 0.50	2.93 ± 0.40
Other mechanisms	0.12 ± 0.04	0.15 ± 0.05‡	0.11 ± 0.04	0.13 ± 0.04

Values are mean ± SD. The function of SERCA significantly reduced following 150 days AC and was further reduced in myocytes from ACOV compared with Sham and AC, respectively. The rate of NCX remained unaltered among groups but contributed more toward Ca^{2+} efflux in the AC groups compared with Sham. The notation describing p values is as follows: *p < 0.001, when comparisons were made with the Sham group. When comparisons were made with the ACOV group, the notation describing p values is †p < 0.05, and ‡p < 0.01.

AC = aortic constriction; ACOV = aortic constriction with ovariectomy; ACOV+E = aortic constriction with ovariectomy supplemented with 17 β -estradiol; NCX = $\text{Na}^+/\text{Ca}^{2+}$ exchange; SERCA = sarco/endoplasmic reticulum Ca^{2+} -ATPase

amplitudes were observed in the ACOV group compared with the Sham, and when estrogen was supplemented (ACOV+E), the size of the amplitude was restored to that of the AC group (Figure 1B).

QUANTIFYING TOTAL SR Ca^{2+} CONTENT. A key feature of heart failure is weak contractile force that is directly correlated with both the amplitude of the Ca^{2+} transient and the total amount of Ca^{2+} within the SR (19–22). We used voltage clamp to maintain the membrane potential of the myocytes at -80 mV while rapidly superfusing the cells with normal Tyrode's solution containing 10 mM caffeine. The rapid and continual application of caffeine results in sustained RyR2-mediated Ca^{2+} release, inducing an inward "forward-mode" $\text{Na}^+/\text{Ca}^{2+}$ exchange (NCX) current (I_{NCX}), and the integral of this current was used to calculate the Ca^{2+} content of the SR, based on the assumptions that all the SR Ca^{2+} was released during the caffeine application and the stoichiometry of the exchange is $3\text{Na}^+:\text{Ca}^{2+}$. The SR Ca^{2+} content significantly decreased by 40% in heart failure compared with Sham and was further reduced by 13% in myocytes from ACOV compared with AC (p < 0.05) (Figure 1C).

INTRACELLULAR Ca^{2+} REMOVAL MECHANISMS. A single-exponential equation was fit to the decay of the Ca^{2+} transient during steady-state stimulation to calculate the total decay rate constant and pooled data are shown in Figure 1D. Myocytes isolated from AC animals had slower transient decay (p < 0.001) compared with Sham. The rate of Ca^{2+} decay was further reduced in myocytes from ovariectomized animals (ACOV) compared with Sham and AC, and when 17 β -estradiol was supplemented, these myocytes had comparable Ca^{2+} decay rates with the AC group (Figure 1D).

Caffeine-induced Ca^{2+} transient protocols (14) were used to differentiate the rates of the cytosolic Ca^{2+} removal mechanisms (Table 2). Sarco/endoplasmic reticulum (SERCA) function significantly decreased following AC and remained low in all AC groups compared with myocytes isolated from Sham. When the SR was removed from Ca^{2+} regulation, the rate of Ca^{2+} decline remained unaltered among groups (Table 2).

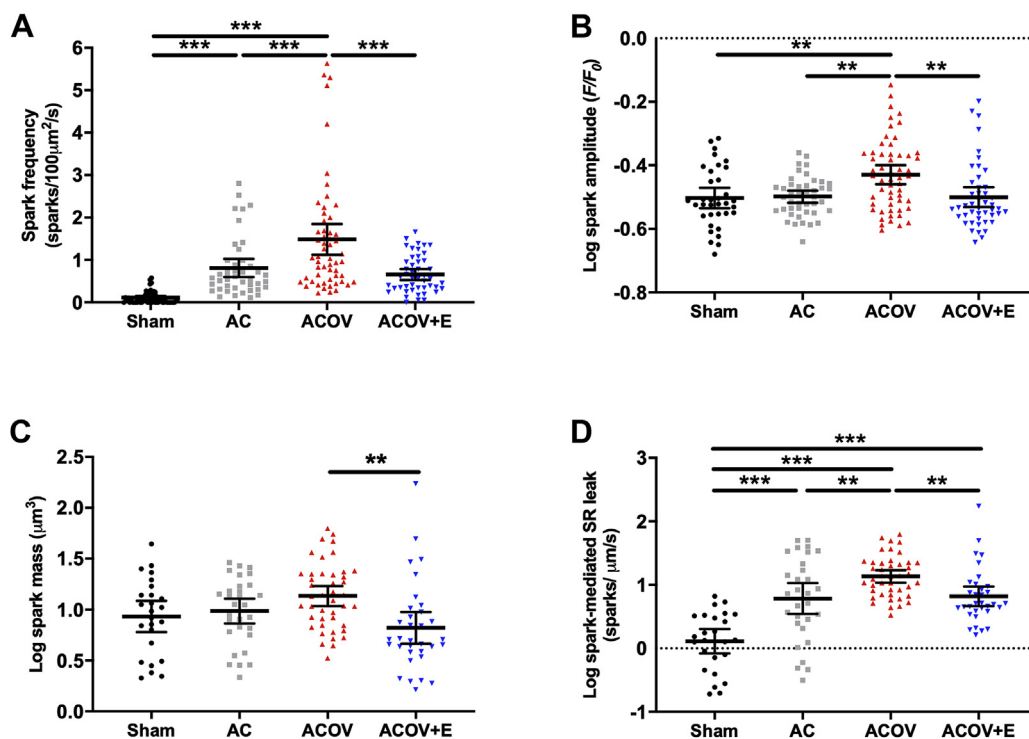
Ca^{2+} SPARK ASSESSMENT. As there is evidence that RyR2-mediated Ca^{2+} release is altered in heart failure (23–26), we measured the occurrence of spontaneous Ca^{2+} sparks. Myocytes from the failing hearts had significantly higher frequency of Ca^{2+} sparks compared with Sham (p < 0.001). In ACOV, Ca^{2+} spark frequency was further increased compared with AC and restored following 17 β -estradiol supplementation (Figure 2). There were no differences in Ca^{2+} spark amplitudes in the AC groups compared with Sham, except for myocytes isolated from ACOV, in which the amplitudes were increased. Calculating the spark-mediated SR leak, by multiplying spark mass by frequency, revealed that myocytes from ACOV had greater SR leak compared with AC and ACOV+E. Myocytes from the failing hearts were characterized by increased spark-mediated SR leak compared with Sham (p < 0.001), correlating with total SR Ca^{2+} content shown in Figure 1.

CARDIAC ACTION POTENTIAL DURATION. Action potential time to 90% repolarization (APD_{90}) was prolonged in the AC groups compared with Sham (p < 0.001) (Figure 3). Unlike other parameters, the long-term absence of ovarian hormones did not further prolong APD_{90} compared with AC, although when animals were supplemented with estrogen (ACOV+E), APD_{90} shortened compared with ACOV (p < 0.01).

INTRACELLULAR Na^+ REGULATION. We have shown that pressure overload and the long-term absence of ovarian hormones results in changes to intracellular Ca^{2+} regulation. Intracellular Ca^{2+} regulation is intertwined with intracellular Na^+ regulation; therefore, we investigated to determine whether important Na^+ efflux and influx routes, known to be altered in heart failure, were affected by ovarian hormone withdrawal. We measured the Na^+/K^+ ATPase current and the late Na^+ current ($I_{\text{Na,Late}}$) in myocytes isolated from each experimental cohort.

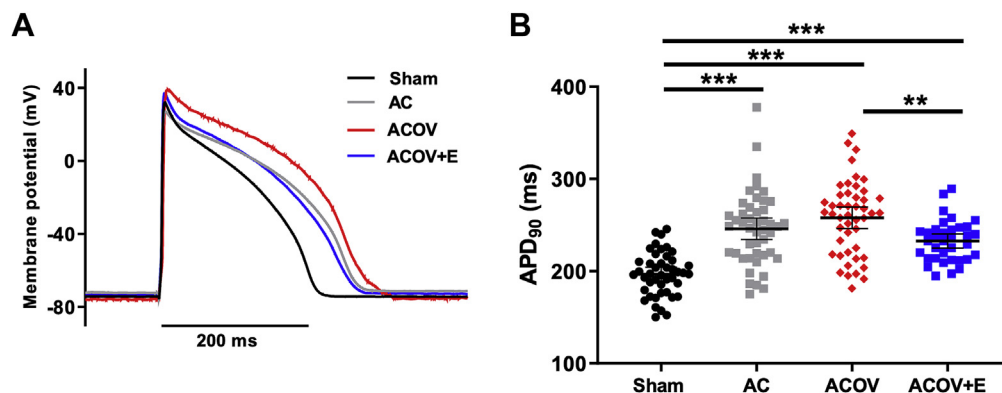
Na^+/K^+ ATPase CURRENT AND REACTIVATION. The protocol for these experiments is illustrated in Figure 4A and is described in detail in Ke et al. (14). Briefly, the Na^+/K^+ ATPase was inhibited by

FIGURE 2 Quantification of Ca^{2+} Spark Frequency and Morphology



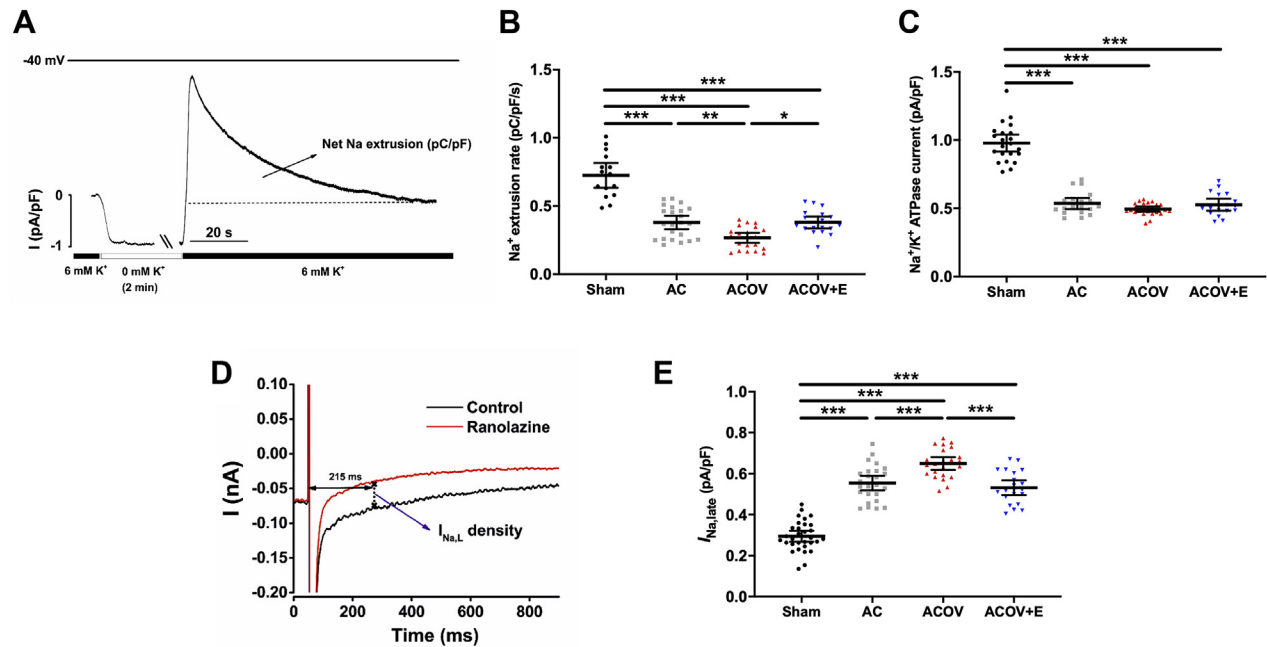
(A) The frequency of Ca^{2+} sparks increased in myocytes from the AC groups and was highest in the ACOV group compared with Sham. The frequency in ACOV+E group is more comparable with the Sham group. (B) The amplitude of the Ca^{2+} spark was similar between the Sham and the AC group. Myocytes from ACOV had the largest Ca^{2+} spark amplitude between groups. (C) Spark mass in ACOV+E group is lower compared with ACOV. (D) The spark-mediated SR leak (spark mass x frequency) increased in all AC groups compared with Sham, with ACOV having the highest leak. (Sham, $n = 57/5$; AC, $n = 43/3$; ACOV, $n = 56/4$; ACOV+E, $n = 47/3$; 1-way ANOVA with a Fisher post hoc test, * $p < 0.05$, ** $p < 0.01$, *** $p < 0.001$). Bars show mean (95% confidence interval). Abbreviations as in Figure 1.

FIGURE 3 Action Potential Duration Time to 90% Repolarization (APD_{90})



(A) Representative action potential traces. (B) APD_{90} was prolonged in all AC groups compared with Sham. The ACOV mean APD_{90} was 23.6% longer than Sham. Sham $n = 44/5$, AC, $n = 46/5$, ACOV $n = 47/3$, ACOV+E $n = 35/3$; 1-way ANOVA with Tukey's multiple comparisons test, ** $p = 0.01$, *** $p < 0.001$. Bars show mean (95% confidence interval). Abbreviations as in Figure 1.

FIGURE 4 Evaluation of Na^+ Influx and Efflux Kinetics



(A) Representative trace of Na^+/K^+ ATPase current alterations when the superfusate was changed from 6 mM K^+ to a K^+ -free solution to inhibit the Na^+/K^+ ATPase and then following the reintroduction of 6 mM K^+ to reactivate the pump. (B) The Na^+/K^+ ATPase-mediated Na^+ extrusion rate following pump reactivation and (C) the total Na^+/K^+ ATPase current density. The Na^+ efflux through Na^+/K^+ ATPase current density and Na^+ extrusion rate were reduced in AC groups. The long-term absence of ovarian hormones resulted in a further reduction in Na^+ extrusion rate compared with the AC group. (Sham, $n = 22/2$; AC, $n = 19/3$; ACOV, $n = 25/2$; ACOV+E, $n = 27/2$; 1-way ANOVA with a Tukey's multiple comparisons test, * $p < 0.05$, *** $p < 0.001$). (D) Na^+ influx through the ranolazine-sensitive late Na^+ current ($I_{\text{Na,L}}$) in myocytes isolated from AC groups. (E) The $I_{\text{Na,L}}$ was increased in AC groups, ACOV had a 15 % greater $I_{\text{Na,L}}$ -related Na^+ influx compared with AC. The estradiol-supplemented group had similar Na^+ influx compared with AC. (Sham, $n = 31/3$; AC, $n = 25/3$; ACOV, $n = 23/3$; ACOV+E, $n = 21/3$; 1-way ANOVA with a Tukey's multiple comparisons test, * $p < 0.05$, *** $p < 0.001$). Bars show mean (95% confidence interval). Abbreviations as in Figure 1.

superfusion of the cells in K^+ -free solution for 2 min, during which time intracellular Na^+ concentration will increase. After 2 min, the superfusate was switched to normal Tyrode's solution that contained 6 mM K^+ . This reactivates the Na^+/K^+ ATPase, which extrudes the accumulated Na^+ from the cell, and the rate of extrusion was used to assess its function. Steady-state Na^+/K^+ ATPase current density was taken as the difference between the holding current in the presence and absence of K^+ .

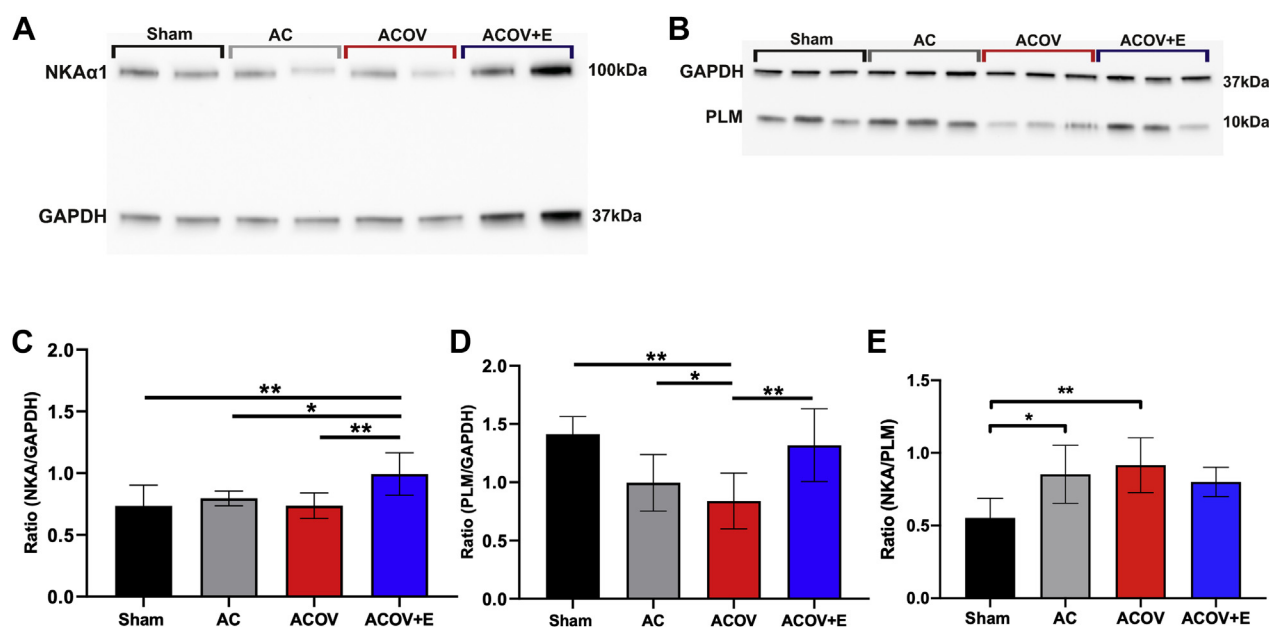
The Na^+ extrusion rate (typical changes in current are shown Figure 4A) was significantly reduced in AC groups compared with Sham ($p < 0.001$), and myocytes from ACOV were characterized by a further reduction in extrusion rate, compared with the AC group, respectively ($p < 0.05$) (Figure 4B). The Na^+/K^+ ATPase current density was reduced by approximately 50% in all AC groups compared with myocytes from Sham ($p < 0.001$) (Figure 4C).

LATE Na^+ CURRENT. Myocyte transmembrane potential was initially clamped at -120 mV before

stepping the membrane potential to -20 mV for 2 s to elicit the $I_{\text{Na,Late}}$, as shown in Figure 4D. The ranolazine-sensitive $I_{\text{Na,Late}}$ was measured 215 ms following the voltage step (27) and compared among groups. Myocytes from the AC groups were collectively characterized by an approximate 100% increase in $I_{\text{Na,Late}}$ compared with the Sham group ($p < 0.001$). The ACOV group had the largest $I_{\text{Na,Late}}$ compared with AC and the ACOV+E groups ($p < 0.001$), and this result was consistent with the increase in charge density, as shown in Figure 4E. Inactivation of the $I_{\text{Na,Late}}$ was prolonged in all AC groups compared with Sham ($p < 0.001$), and the speed of inactivation was independent of the AC experimental group.

These experiments present evidence of a decline in Na^+/K^+ ATPase current and Na^+ extrusion as the heart begins to fail. To assess if the decline in these 2 indices of function may be explained by a decrease in the amount of pump protein or its regulatory subunit phospholemman (PLM/FXYD1), we undertook Western-blotting experiments (Figure 5). Although

FIGURE 5 Na^+/K^+ ATPase and Its Regulatory Subunit Expression



(A) A sample Western blot of Na^+/K^+ ATPase (NKA) $\alpha 1$ expression in Sham and AC groups with the grouped data (C). The Na^+/K^+ ATPase $\alpha 1$ relative expression was unchanged in the AC groups compared with Sham, except for the ACOV+E group, in which the ratio was 25.9% greater. (B) A sample Western blot of phospholemman (PLM/FXYD1) expression in Sham and AC groups with the grouped data (D). Phospholemman expression decreases in the ACOV group, but supplementation with estradiol increases expression to match Sham levels, with the ACOV+E ratio 36% greater than ACOV expression. (E) The ratio of the expression levels of the 2 proteins (Na^+/K^+ ATPase: PLM) in the AC and ACOV cohorts increased compared with Sham. $N = 6$ for each group; 1-way ANOVA with a Fisher post hoc test, * $p < 0.05$, ** $p < 0.01$. Bars show mean \pm SD. Abbreviations as in Figure 1.

the expression of Na^+/K^+ ATPase $\alpha 1$ subunit (NKA $\alpha 1$) was not different, except for the AVOV+E group, in which the ratio was greater compared with Sham (Figures 5A and 5C), the amount of PLM decreased in ACOV compared with the other groups (Figures 5B and 5D). The lower expression level of regulatory inhibitory subunit could increase Na^+/K^+ ATPase function because unphosphorylated PLM inhibits the Na^+/K^+ ATPase. We found the ratio of the expression levels of the 2 proteins (Na^+/K^+ ATPase: PLM) in each experimental cohort to increase in the disease states compared with Sham (Figure 5E), suggesting that levels of the phosphorylated form of PLM could be more important in determining Na^+/K^+ ATPase function, or interactions between the Na^+/K^+ ATPase and PLM are altered.

DISCUSSION

The aim of this work was to characterize the influence of estrogen on cardiac function during the onset of heart failure in a controlled animal model that lacks traditional comorbidities. As well as assessing the effect of estrogen on in vivo cardiac function, we

investigated its possible effects on intracellular Ca^{2+} and Na^+ regulation, as these 2 ions play major roles in determining cardiac contractility, and their cellular homeostasis is known to change in heart failure. Four experimental animal groups were produced to test the hypothesis that long-term absence of ovarian hormones is detrimental to cardiac function and that such deleterious effects can be rescued by 17 β -estradiol. The guinea pig offers a useful animal model because the species shares similar electrophysiological, Ca^{2+} regulatory, and steroidogenesis features with humans (13).

HEART FAILURE AND OVARECTOMY. Aortic constriction progresses in males of this species to the presentation of heart failure with reduced ejection fraction (HFrEF) approximately 150 days later (Sham mean EF = 73%, HF mean = 37%) (14). Significant cardiac hypertrophy develops with an enlargement of the diastolic internal left-ventricular diameter, indicating volume retention in the left chambers that produces pulmonary congestion, confirmed by the increased LW:BW. A duplication of the procedure in female animals in this paper

also causes a decrease in EF, indicating that systolic function is affected.

Ventricular myocytes isolated from the female failing hearts had reduced Ca^{2+} transient amplitudes that, given the unaltered fractional SR Ca^{2+} release, are a likely consequence of the decrease in SR Ca^{2+} content. The reduced amplitude of the Ca^{2+} transient combined with a reduction in myofilament sensitivity that accompanies a reduction in estrogen (9) will contribute to worse diastolic dysfunction compared with the AC group and correlates well with the increase in left-ventricular chamber dimensions during systole (LVIDs), indicating weaker *in vivo* contractile force and reduced fractional shortening.

The slower transient decay kinetics indicates that cytosolic Ca^{2+} removal systems are less effective. Although declining SERCA function is well known in heart failure and results in reduced SR Ca^{2+} content, our other measurements point to altered intracellular Na^+ regulation in heart failure that will affect the function of the $\text{Na}^+/\text{Ca}^{2+}$ exchange. The reduction in Na^+/K^+ ATPase current and Na^+ extrusion rate lead to an increase in intracellular $[\text{Na}^+]$ aggravated by the increase in Na^+ influx via $I_{\text{Na,late}}$ that will contribute to a prolongation of the action potential. These changes will alter the balance of Ca^{2+} flux generated by the $\text{Na}^+/\text{Ca}^{2+}$ exchange, reducing its forward mode, slowing cytosolic Ca^{2+} removal during the cardiac cycle. It is likely that the reduced whole heart function, reduction in myocyte SR Ca^{2+} contents, and Ca^{2+} transients are partly offset by the increase in intracellular $[\text{Na}^+]$ reported in other heart-failure models (28–30) and in human (31,32). We have suggested that the increase in inward Na^+ flux and the decrease in Na^+/K^+ ATPase current and function alters the balance of Ca^{2+} flux mediated by the $\text{Na}^+/\text{Ca}^{2+}$ exchange during the cardiac cycle that limits early contractile impairment (14).

One hundred-fifty days following ovariectomy, uterine weight and serum estradiol levels had significantly decreased in the ACOV group, confirming a long-term absence of ovarian hormones and in line with our published ovariectomy results (8). Following ovariectomy, failing hearts showed additional impairment of global function, and their ventricular myocytes displayed further deterioration of cellular Ca^{2+} regulation compared with the gonad-intact heart failure group. When these animals received 17β -estradiol, the global and cellular functional indicators improved to match the values of the gonad-intact heart failure group. Other work, using animal models of cardiac pathology that provided estrogen supplementation, supports these observations. Some studies find that the development of

ventricular hypertrophy is slowed (33,34); reversed (35); or there are different effects, depending on the type of pathological insult (36).

These other studies were limited to descriptions of whole heart function and morphology. Here we describe not only global changes occurring in response to estrogen supplementation following pressure overload but also concurrent alterations to myocyte Ca^{2+} and Na^+ regulation. To our knowledge this is the first time such studies have been described, and they suggest that estrogen can modulate ventricular myocyte responses to heart failure and, more specifically, the function of proteins involved in intracellular ionic regulation.

Knowledge of the underlying mechanisms is scant and much more exploration will be required to improve our understanding of them (37). There is evidence that they may involve estrogen receptor α ($\text{ER}\alpha$) and its interaction with nuclear factor (NF)- κB in modulating estrogen-dependent transcriptional regulation (38,39); and/or G-protein-coupled estrogen receptor-1 (GPER1 or GPR30), as its activation has been reported to reduce infarct size and improve function following ischemia/reperfusion (40); inhibiting the translocation of the hypertrophic transcription factor, NF-AT, to the nucleus of the cardiac myocyte; and stimulating NF-AT transcriptional activity (41). Cardiac-specific overexpression of $\text{ER}\alpha$ may protect female mouse hearts following myocardial infarction induced by coronary artery ligation through encouraging angiogenesis and reducing fibrosis, but the effects of overexpression of ERs or the effects mediated by ERs on Ca^{2+} regulation are largely unknown (39). In smooth muscle, GPER1 may be involved in the regulation of intracellular Ca^{2+} by voltage-sensitive channels (42) and in the kidney appears to mediate changes in Ca^{2+} signaling that do not occur in GPER1 knockout mice (43). It has also been observed that overexpression of $\text{ER}\beta$ improves cardiac function following infarction (44), and both receptors have been implicated in suppressing isoprenaline-induced cardiac hypertrophy (45,46).

ESTROGEN EFFECTS ON THE CHANGES TO ELECTROPHYSIOLOGY. The spark-mediated SR leak was greater in the dual-surgery (ACOV) group compared with AC group. This may partly explain the smaller SR Ca^{2+} content in the former group (47) and could be proarrhythmic because larger spontaneous Ca^{2+} release events will activate the NCX that, in turn, may lead to the formation of after-depolarizations. Ca^{2+} spark frequency is dependent on SR Ca^{2+} content, and at least part of the reduced SR Ca^{2+} content

is undoubtedly caused by the enhanced leak that may be spark mediated or by other routes (48).

Activated exchange current may contribute to the action potential prolongation and may increase the potential for re-excitation. A key feature of heart failure is prolongation of the cardiac action potential, and we have suggested in this animal model that an increase in Na^+ influx via $I_{\text{Na,late}}$ is involved (14). Strikingly, the absence of estrogen in heart failure further increases $I_{\text{Na,late}}$ and further prolongs the APD compared with heart failure when estrogen is present. The role of estrogen in arrhythmias is controversial (49), but this result indicates that estrogen alters the function of ion channels that control cardiac excitation and repolarization.

STUDY LIMITATIONS. The Ca^{2+} transient measurements are qualitative rather than quantitative, and we do not know if changes to cellular Ca^{2+} buffering occur. Given the nonlinear relationship between free $[\text{Ca}^{2+}]_i$ and fluxes this imposes limitations on some of the interpretations of our data, notably the comparison of rate constants, which can only be done over similar ranges of free $[\text{Ca}^{2+}]_i$.

CONCLUSIONS

Many of the changes to global and cellular functions that take place during the onset of heart failure were made worse following reduction of circulating levels of ovarian hormones by ovariectomy. The worsening of function could be counteracted with 17β -estradiol supplementation, suggesting that estrogens play a role in the adaptive and maladaptive responses occurring during the onset of heart failure.

ACKNOWLEDGMENTS The authors acknowledge use of the Imperial College Facility for Imaging by Light Microscopy (FILM) and thank Dr. Tristan Rodriguez's group for technical assistance and use of their Criterion Cell midi-format chamber for electrophoresis and Western blot.

ADDRESS FOR CORRESPONDENCE: Dr. Kenneth T. MacLeod, National Heart and Lung Institute, Imperial Centre for Translational and Experimental Medicine (ICTEM), Imperial College, Hammersmith Hospital, Du Cane Road, London W12 0NN, United Kingdom. E-mail: k.t.macleod@imperial.ac.uk.

PERSPECTIVES

COMPETENCY IN MEDICAL KNOWLEDGE: The myocardial actions of sex steroids are complex, but evidence is emerging that suggests they may be beneficial in specific situations. The challenge is to determine the mechanisms whereby sex steroids affect electrophysiological and Ca^{2+} homeostasis remodeling of the cardiac myocyte, ultimately improving lusitropic function and reducing proarrhythmic substrate. A better understanding of the mechanisms involved will influence a more tailored—and therefore more effective—approach to treatment strategies for female patients that may, in the longer term, benefit both sexes. Here, we describe not only beneficial global changes occurring in response to estrogen supplementation following pressure overload but also concurrent improvements to cardiac myocyte Ca^{2+} regulation. The results support the view that estrogen supplementation can influence cardiac remodeling, improving function at whole-heart and cellular levels.

TRANSLATIONAL OUTLOOK: Cardiomyocytes express sarcolemmal- and nuclear-bound estrogen receptors $\text{ER}\alpha$ and $\text{ER}\beta$, and GPER; however, their influence on mechanisms and processes involved in excitation-contraction coupling and ionic regulation are essentially unexplored. It would be tempting to suggest that 17β -estradiol directly interacts with estrogen receptors on the cardiomyocyte membrane, eliciting downstream signaling cascades that modulate ion channel/transporter/exchanger function. Future studies would need to pinpoint the receptors involved, tailoring toward gender-specific therapy.

REFERENCES

1. Humphries KH, Izadnegahdar M, Sedlak T, et al. Sex differences in cardiovascular disease: impact on care and outcomes. *Front Neuroendocrinol* 2017;46:46-70.
2. Regitz-Zagrosek V, Kararigas G. Mechanistic pathways of sex differences in cardiovascular disease. *Physiol Rev* 2016;97:1-37.
3. Crandall CJ, Barrett-Connor E. Endogenous sex steroid levels and cardiovascular disease in relation to the menopause: a systematic review. *Endocrinol Metab Clin* 2013;42:227-53.
4. Mendelsohn ME, Karas RH. The protective effects of estrogen on the cardiovascular system. *N Engl J Med* 1999;340:1801-11.
5. Rossouw JE, Anderson GL, Prentice RL, et al. Risks and benefits of estrogen plus progestin in healthy postmenopausal women: principal results from the women's health initiative randomized controlled trial. *J Am Med Assoc* 2002;288:321-33.
6. Gersh FL, Lavie CJ. Menopause and hormone replacement therapy in the 21st century. *Heart* 2020;106:479-81.
7. Muka T, Oliver-Williams C, Kunutsor S, et al. Association of age at onset of menopause and time since onset of menopause with cardiovascular outcomes, intermediate vascular traits, and all-cause mortality: a systematic review and meta-analysis. *JAMA Cardiol* 2016;1:767-76.
8. Yang HY, Firth JM, Francis AJ, Alvarez-Laviada A, MacLeod KT. Effect of ovariectomy on intracellular Ca^{2+} regulation in guinea pig cardiomyocytes. *Am J Physiol* 2017;313:H1031-43.
9. Fares D, Pyle WG, Ray G, Denovan-Wright EM, Chen RP, Howlett SE. The impact of ovariectomy

on calcium homeostasis and myofilament calcium sensitivity in the aging mouse heart. *PLoS One* 2013;8:e74719.

10. Fares E, Parks RJ, MacDonald JK, Egar JMS, Howlett SE. Ovariectomy enhances SR Ca^{2+} release and increases Ca^{2+} spark amplitudes in isolated ventricular myocytes. *J Mol Cell Cardiol* 2012;52:32-42.

11. Wang Y, Wang Q, Zhao Y, et al. Protective effects of estrogen against reperfusion arrhythmias following severe myocardial ischemia in rats. *Circ J* 2010;74:634-43.

12. Sourander L, Rajala T, R  ih   I, M  kinen J, Erkkola R, Helenius H. Cardiovascular and cancer morbidity and mortality and sudden cardiac death in postmenopausal women on oestrogen replacement therapy (ERT). *Lancet* 1998;352:1965-9.

13. Taggart MJ, Hume R, Lartey J, Johnson M, Tong WC, MacLeod KT. Cardiac remodelling during pregnancy: whether the guinea pig? *Cardiovasc Res* 2014;104:226-7.

14. Ke HY, Yang HS, Francis AJ, et al. Changes in cellular Ca^{2+} and Na^{+} regulation during the progression towards heart failure in the guinea pig. *J Physiol* 2020;598:1339-59.

15. MacLeod KT, Harding SE. Effects of phorbol ester on contraction, intracellular pH and intracellular Ca^{++} in isolated mammalian ventricular myocytes. *J Physiol* 1991;444:481-98.

16. Sikkil M, Collins T, Rowlands C, et al. Flecainide reduces Ca^{2+} spark and wave frequency via inhibition of the sarcolemmal sodium current. *Cardiovasc Res* 2013;98:286-96.

17. Picht E, Zima AV, Blatter LA, Bers DM. SparkMaster: automated calcium spark analysis with ImageJ. *Am J Physiol* 2007;293:C1073-81.

18. Hollingworth S, Peet J, Chandler WK, Baylor SM. Calcium sparks in intact skeletal muscle fibers of the frog. *J Gen Physiol* 2001;118:653-78.

19. Beuckelmann DJ, N  bauer M, Erdmann E. Intracellular calcium handling in isolated ventricular myocytes from patients with terminal heart failure. *Circulation* 1992;85:1046-55.

20. Hasenfuss G, Reinecke H, Studer R, et al. Relation between myocardial function and expression of sarcoplasmic reticulum Ca^{2+} -ATPase in failing and nonfailing human myocardium. *Circ Res* 1994;75:434-42.

21. Hasenfuss G, Reinecke H, Studer R, et al. Calcium cycling proteins and force-frequency relationship in heart failure. *Basic Res Cardiol* 1996;91 suppl 2:17-22.

22. Piacentino V III, Weber CR, Chen X, et al. Cellular basis of abnormal calcium transients of failing human ventricular myocytes. *Circ Res* 2003;92:651-8.

23. Litwin SE, Zhang D, Bridge JHB. Dyssynchronous Ca^{2+} sparks in myocytes from infarcted hearts. *Circ Res* 2000;87:1040-7.

24. Marks AR. Ryanodine receptors/calcium release channels in heart failure and sudden cardiac death. *J Mol Cell Cardiol* 2001;33:615-24.

25. Marx SO, Reiken S, Hisamatsu Y, et al. PKA phosphorylation dissociates FKBP12.6 from the calcium release channel (ryanodine receptor): defective regulation in failing hearts. *Cell* 2000;101:365-76.

26. Shannon TR, Pogwizd SM, Bers DM. Elevated sarcoplasmic reticulum Ca^{2+} leak in intact ventricular myocytes from rabbits in heart failure. *Circ Res* 2003;93:592-4.

27. Maltsev VA, Sabbah HN, Higgins RSD, Silverman N, Lesch M, Androvinas AI. Novel, ultraslow inactivating sodium current in human ventricular cardiomyocytes. *Circulation* 1998;98:2545-52.

28. Despa S, Islam MA, Weber CR, Pogwizd SM, Bers DM. Intracellular Na^{+} concentration is elevated in heart failure but $\text{Na}^{+}/\text{K}^{+}$ pump function is unchanged. *Circulation* 2002;105:2543-8.

29. Baartscheer A, Schumacher CA, van Borren MMGJ, Belterman CNW, Coronel R, Fiolet JWT. Increased $\text{Na}^{+}/\text{H}^{+}$ -exchange activity is the cause of increased $[\text{Na}^{+}]_{i}$ and underlies disturbed calcium handling in the rabbit pressure and volume overloaded heart failure model. *Cardiovasc Res* 2003;57:1015-24.

30. Schillinger W, Teucher N, Christians C, et al. High intracellular Na^{+} preserves myocardial function at low heart rates in isolated myocardium from failing hearts. *Eur J Heart Fail* 2006;8:673-80.

31. Gray RP, McIntyre H, Sheridan DS, Fry CH. Intracellular sodium and contractile function in hypertrophied human and guinea-pig myocardium. *Pfl  gers Arch* 2001;442:117-23.

32. Pieske B, Maier LS, Piacentino V III, Weisser J, Hasenfuss G, Houser SR. Rate dependence of $[\text{Na}^{+}]_{i}$ and contractility in nonfailing and failing human myocardium. *Circulation* 2002;106:447-53.

33. van Eickels M, Grohe C, Cleutjens JPM, Janssen BJ, Wellens HJJ, Doevendans PA. 17  -estradiol attenuates the development of pressure-overload hypertrophy. *Circulation* 2001;104:1419-23.

34. Westphal C, Schubert C, Prella K, et al. Effects of estrogen, an ER   agonist and raloxifene on pressure overload induced cardiac hypertrophy. *PLoS One* 2012;7:e50802.

35. Cui YH, Tan Z, Fu XD, Xiang QL, Xu JW, Wang TH. 17beta-estradiol attenuates pressure overload-induced myocardial hypertrophy through regulating caveolin-3 protein in ovariectomized female rats. *Mol Biol Rep* 2011;38:4885-92.

36. Patten RD, Pourati I, Aronovitz MJ, et al. 17 Beta-estradiol differentially affects left ventricular and cardiomyocyte hypertrophy following myocardial infarction and pressure overload. *J Card Fail* 2008;14:245-53.

37. Murphy E. Estrogen signaling and cardiovascular disease. *Circ Res* 2011;109:687-96.

38. Mahmoodzadeh S, Fritschka S, Dworatzek E, et al. Nuclear factor-kappaB regulates estrogen

receptor-alpha transcription in the human heart. *J Biol Chem* 2009;284:24705-14.

39. Mahmoodzadeh S, Leber J, Zhang X, et al. Cardiomyocyte-specific estrogen receptor alpha increases angiogenesis, lymphangiogenesis and reduces fibrosis in the female mouse heart post-myocardial infarction. *J Cell Sci Ther* 2014;5:153-68.

40. Deschamps AM, Murphy E. Activation of a novel estrogen receptor, GPER, is cardioprotective in male and female rats. *Am J Physiol* 2009;297:H1806-13.

41. Pedram A, Razandi M, Aitkenhead M, Levin ER. Estrogen inhibits cardiomyocyte hypertrophy in vitro: antagonism of calcineurin-related hypertrophy through induction of MCIP1. *J Biol Chem* 2005;280:26339-48.

42. Holm A, Hellstrand P, Olde B, Svensson D, Leeb-Lundberg LM, Nilsson BO. The G protein-coupled estrogen receptor 1 (GPER/GPR30) agonist G-1 regulates vascular smooth muscle cell Ca^{2+} handling. *J Vasc Res* 2013;50:421-9.

43. Hofmeister MV, Damkier HH, Christensen BM, et al. 17beta-estradiol induces nongenomic effects in renal intercalated cells through G protein-coupled estrogen receptor 1. *Am J Physiol* 2012;302:F358-68.

44. Schuster I, Mahmoodzadeh S, Dworatzek E, et al. Cardiomyocyte-specific overexpression of oestrogen receptor    improves survival and cardiac function after myocardial infarction in female and male mice. *Clin Sci* 2016;130:365.

45. Fang HY, Hung MY, Lin YM, et al. 17  -Estradiol and/or estrogen receptor alpha signaling blocks protein phosphatase 1 mediated ISO induced cardiac hypertrophy. *PLoS One* 2018;13:e0196569.

46. Tsai CY, Kuo WW, Shibu MA, et al. E2/ER    inhibit ISO-induced cardiac cellular hypertrophy by suppressing Ca^{2+} -calcineurin signaling. *PLoS One* 2017;12:e0184153.

47. Bers DM, Eisner DA, Valdivia HH. Sarcoplasmic reticulum Ca^{2+} and heart failure: roles of diastolic leak and Ca^{2+} transport. *Circ Res* 2003;93:487-90.

48. Zima AV, Bovo E, Bers DM, Blatter LA. Ca^{2+} spark-dependent and -independent sarcoplasmic reticulum Ca^{2+} leak in normal and failing rabbit ventricular myocytes. *J Physiol* 2010;588:4743-57.

49. Iorga A, Cunningham CM, Moazeni S, Ruffenach G, Umar S, Eghbali M. The protective role of estrogen and estrogen receptors in cardiovascular disease and the controversial use of estrogen therapy. *Biol Sex Differ* 2017;8:33.

KEY WORDS calcium regulation, cardiomyocytes, excitation-contraction coupling, estrogen, female, heart failure

APPENDIX For supplemental material, please see the online version of this paper.